EPJ Web of Conferences **66**, 03008 (2014)
DOI: 10.1051/epjconf/ 2014 6603008

Breakup, fusion, and elastic scattering analysis of the ^{8}B + ^{58}Ni system at low energies with the continuum-discretized coupled channels method

T. L. Belyaeva [1a], P. Amador-Valenzuela[1,2], E. F. Aguilera[2], E. Martinez-Quiroz[2], and J. J. Kolata[3]

[1]Universidad Autónoma del Estado de México, C. P. 50000, Toluca, México
[2]Depto. de Aceleradores, Instituto Nacional de Investigaciones Nucleares, A. P. 18-1027, C. P. 11801 México, D. F., México
[3]Physics Department, University of Notre Dame, Notre Dame, Indiana, 46556, USA

Abstract. We have performed continuum-discretized coupled channels (CDCC) calculations of the breakup of ^{8}B on ^{58}Ni in the energy interval 10 – 26 MeV in the c.m. system. Elastic scattering angular distributions for the ^{8}B + ^{58}Ni system at five different energies around the Coulomb barrier were studied by using the CDCC model and taking into account a coupling between elastic and breakup channels. The energy-dependent sets found for the OPs parameters reproduce well the elastic scattering data and the fusion and reaction cross sections. Finally, a comparison of the reduced total reaction cross sections for the ^{8}B + ^{58}Ni system with the ^{6}He + ^{208}Pb and ^{6}He + ^{209}Bi systems is presented.

1 Introduction

The study of nuclear reactions induced by radioactive beams of nuclei located near the neutron or proton drip lines reveals interesting new phenomena such as the formation of halo structures [1, 2]. The presence of halo structure means that an rms matter radius is larger than the usual value deduced from the $r_0A^{1/3}$–systematics and a dilute nuclear density appears in an enlarged peripheral region. The low binding energies of the valence nucleons result in increased probabilities for such reaction channels as nucleon transfer, breakup and fusion, especially in the sub-barrier energy region. The competition and/or coupling between these reaction mechanisms for drip-line nuclei are of great interest and have been raised recently in many experimental and theoretical studies (see, e.g. [3], for details).

One of the best-studied two-neutron halo nuclei is ^{6}He. To elucidate the specific effects of the halo, its interaction with heavy targets at around-barrier energies has been compared with reactions induced by ^{4}He, the nucleus that represents the core of ^{6}He [4–7]. It was shown that the sum of the fusion plus ‘‘breakup/transfer’’ yields saturates the total reaction cross section predicted from an analysis of simultaneously measured elastic scattering angular distributions. A systematic study of total reaction cross sections for ^{6}He and ^{4}He projectiles performed in Ref. [8, 9] has shown that the reduced cross sections for both projectiles follow well-defined trajectories that can be characterized by respective Wong-type curves. This method used the reduced cross sections $\sigma_{red} = \sigma/(A_p^{1/3} + A_t^{1/3})^2$ and reduced

[a] Corresponding author: tbl@uaemex.mx

energies $E_{red} = E_{c.m.}/[(Z_pZ_t)/(A_p^{1/3} + A_t^{1/3})]$ suggested in [10], in order to make a comparison between different systems. The strong enhancement observed for the ^{6}He data was interpreted as caused by two separate halo effects. The size effect is a geometric effect, related to the extended size of the halo nucleus, which affects the cross sections in the whole energy region. The dynamic effect is important mainly in the energy region near or below the barrier, and it is probably related to the enhanced transfer/breakup processes that were observed for ^{6}He.

Reactions induced by light proton-rich projectiles provide a good possibility to study proton halos. Unlike the neutron-rich systems, the valence proton in the loosely bound proton-rich nuclei has to tunnel through the barrier resulting from the Coulomb repulsion due to the charged core. Thus, a comparison of reaction mechanisms realized in the processes induced by proton-rich and neutron-rich projectiles may provide understanding of the halo phenomenon. For example, reactions induced by the exotic nucleus ^{8}B, which has a weakly bound proton (0.137 MeV), were widely studied both experimentally [11–15] and theoretically [16–21]. In Ref. [8, 9], it was shown that the reduced total reaction cross sections for the proton halo nucleus ^{8}B with different targets, lie on the same trajectory as those for the neutron halo nucleus ^{6}He. This analysis was based on the experimental study of the elastic scattering and total reaction cross section measured for ^{8}B incident on a ^{58}Ni target at several energies near the Coulomb barrier [14]. The fusion excitation function for the ^{8}B + ^{58}Ni system recently measured [15] at nine near-barrier energies showed a striking enhancement with respect to expectations for normal projectiles. The calculations carried out in the continuum–discretized coupled channels (CDCC) method (breakup) and optical model (fusion) [14, 21] presented evidence that the sum of the fusion and breakup yields saturates the total reaction cross section.

We find it interesting to investigate a coupling between breakup, fusion and elastic scattering for the ^{8}B + ^{58}Ni system and how it could affect the total reaction cross section at near barrier energies. In the present work, we report the results of the analysis of the ^{8}B + ^{58}Ni system with the CDCC method in the energy interval 10 – 26 MeV in the c.m. system, which includes energies both below and above the Coulomb barrier ($V_{c.m.}$ = 20.8 MeV).

2 Results and discussion

We carried out the CDCC calculations of the breakup, fusion, and elastic scattering of ^{8}B on ^{58}Ni using the code FRESCO [22] and compared the results with the differential cross sections and the excitation functions measured in Refs. [13–15]. A theoretical analysis within the CDCC method was made for breakup of ^{8}B using a more extended model space as that in [21]: inelastic excitations in the ^{7}Be-proton system from the ground state to excited states with orbital angular momenta L = 0–5 and energies up to 8 MeV in the continuum were taken into account.

Figure 1 shows the experimental data and CDCC calculations for the fusion cross section (σ_{fus}), the total reaction cross section (σ_R), and the breakup plus transfer cross section (σ_{bu+tr}), in reduced form, for the ^{8}B + ^{58}Ni system. The reduced data are expected to eliminate trivial effects of size and charge, thus making data for different systems directly comparable. Figure 1 also shows a comparison of the reduced total reaction cross sections for the ^{8}B + ^{58}Ni system and the ^{6}He + ^{208}Pb [7] and ^{6}He + ^{209}Bi [4–6] systems.

The respective values of σ_{fus} for the ^{8}B + ^{58}Ni system, reported in Ref. [15], were determined from the integrated cross sections for the evaporated protons (σ_p) at energies around the Coulomb barrier by using proton multiplicities (M_p) calculated with the code PACE [23]. The σ_R and σ_{bu} data were reported in Ref. [14] and Ref. [11], respectively.

Our calculations reproduce the experimental fusion and total reaction cross sections and predict the respective behavior at low incident energies. The dashed curve includes full inelastic couplings in the continuum (bu) calculated by the CDCC model plus the direct proton transfer (tr) calculated in the coupled-reaction-channels (CRC) approach. We note that the cross section of proton stripping provides approximately 5% of the total ^{7}Be emission cross sections at $E_{c.m.}$= 22.5 MeV and rapidly decreases for energies below the Coulomb barrier. The dot-dashed curve is a calculation for the fusion assuming that $\sigma_{fus} = \sigma_R - \sigma_{bu+tr}$. One can see that the calculations are in excellent agreement with all

reported data available for σ_{fus}, σ_R, and σ_{bu} at energies around the Coulomb barrier. Even though there are not experimental data available for energies well below the Coulomb barrier, our CDCC calculations show that the breakup is a predominant process for these energies, while fusion becomes more important at energies above the Coulomb barrier.

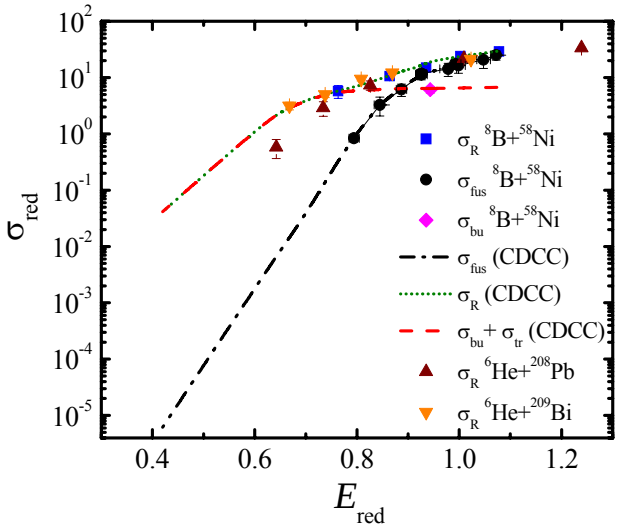

Figure 1. Experimental data for σ_{fus}, σ_R and σ_{bu} in reduced form for the ^{8}B + ^{58}Ni system. The curves were obtained from CDCC calculations for this system, performed with the code FRESCO. A comparison with reduced data for other systems is also shown.

We have already mentioned that the total reaction cross sections for the proton-halo nucleus ^{8}B and the two-neutron-halo nucleus ^{6}He with different targets lie on the same trajectory when plotted in reduced form, despite differences in the structure, binding energy, and reaction mechanisms of these systems [8, 9]. In this context, one can see that the CDCC calculations are also in agreement with the reported σ_R for the ^{6}He + ^{209}Bi system and slightly overestimate σ_R for the ^{6}He + ^{208}Pb system.

In our analysis, we studied the influence of the ^{7}Be core - target optical potential (OP) and p – target OP on the breakup and fusion cross sections. In general, the OP parameters used for the ^{7}Be + ^{58}Ni channel were gathered from Ref. [21] and those for p + ^{58}Ni from the compilation of phenomenological optical-model parameters of Perey and Perey [24]. Adopted OP parameters, for both channels, are energy-dependent. The method used to control this energy dependence was through calculating the volume integrals for the real and imaginary parts of OPs. The real volume integrals were found to be approximately constant (around 360 – 370 MeV fm^3). The imaginary volume integrals go rapidly to zero as the energy decreases below the barrier.

In Figure 2, the ^{8}B + ^{58}Ni elastic-scattering angular distributions measured in Ref. [14] in the angular range $\theta_{c.m.}$ = 25° – 158° for five energies around the Coulomb barrier are shown. Our elastic-scattering calculations (curves), performed by using the CDCC model, took into account a coupling between elastic and breakup channels. The energy-dependent sets found for the OPs parameters reproduce well the elastic scattering data, and the fusion and reaction cross sections.

Finally, we conclude that the CDCC calculations reproduce well the experimental data for the elastic scattering, breakup, fusion, and total reaction cross sections for the ^{8}B + ^{58}Ni system. The sum of the fusion and breakup (plus transfer) yields exhausts the total reaction cross section for this system. We found a considerable coupling between breakup, fusion and elastic scattering and were able to adjust completely the experimental breakup, fusion, and total reaction cross sections in the earlier mentioned energy interval, simultaneously with the ^{8}B + ^{58}Ni elastic scattering differential cross sections. Our results are consistent with the Wong-type calculations of fusion with enlarged barrier radius in comparison with the normal systems [9]. Thus, the CDCC calculations confirm a strong static effect of the ^{8}B proton halo. Comparison of the total cross section calculations of the

reactions induced by proton- and neutron-halo projectiles, ^{8}B on ^{58}Ni and ^{6}He on ^{209}Bi, also showed satisfactory agreement.

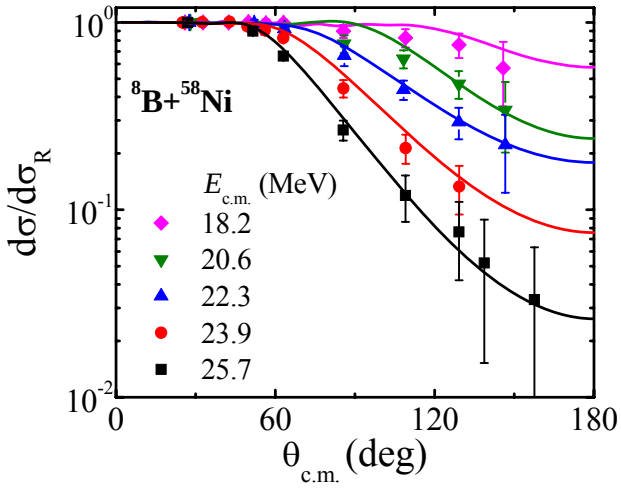

Figure 2. The elastic scattering angular distributions for ^{8}B + ^{58}Ni calculated with the CDCC model (curves), by taking into account a coupling between elastic and bu mechanisms, in comparison with the experimental data [14].

References

1. I. Tanihata *et al.*, Phys. Rev. Lett. **55**, 2676 (1985).
2. P. G. Hansen, A. S. Jensen, and B. Jonson, Ann. Rev. Nucl. Part. Sci. **45**, 591 (1995).
3. B. Jonson, Phys. Rep. **389**, 1 (2004).
4. J. J. Kolata *et al.*, Phys. Rev. Lett. **81**, 4580 (1998).
5. E. F. Aguilera *et al.*, Phys. Rev. Lett. **84**, 5058 (2000).
6. E. F. Aguilera *et al.*, Phys. Rev. C **63**, 061603(R) (2001).
7. A. M. Sánchez-Benítez *et al.*, Nucl. Phys. A **803**, 30 (2008).
8. J. J. Kolata and E. F. Aguilera, Phys. Rev. C **79**, 027603 (2009).
9. E. F. Aguilera, I. Martel, A. M. Sánchez-Benítez, and L. Acosta, Phys. Rev. C **83**, 021601(R) (2011).
10. P. R. S. Gomes, J. Lubian, I. Padron, R. M. Anjos, Phys. Rev. C **71**, 017601 (2005).
11. V. Guimarães *et al.*, Phys. Rev. Lett. **84**, 1862 (2000).
12. J. J. Kolata *et al.*, Phys. Rev. C **63**, 024616 (2001).
13. E. F. Aguilera, E. Martinez-Quiroz, T. L. Belyaeva, J. J. Kolata, and R. Leyte-Gonzalez, Phys. At. Nucl. **71**, 1191 (2008).
14. E. F. Aguilera *et al.*, Phys. Rev. C **79**, 021601(R) (2009).
15. E. F. Aguilera *et al.*, Phys. Rev. Lett. 107, 092701 (2011).
16. F. M. Nunes and I. J. Thompson, Phys. Rev. C **57**, R2818 (1998); **59**, 2652 (1999).
17. H. Esbensen and G. F. Bertsch, Phys. Rev. C **59**, 3240 (1999).
18. J. A. Tostevin, F. M. Nunes, and I. J. Thompson, Phys. Rev. C **63**, 024617 (2001).
19. A. M. Moro and F. M. Nunes, Nucl. Phys. **A767**, 138 (2006).
20. J. Lubian, T. Correa, P. R. S. Gomes, and L. F. Canto, Phys. Rev. C **78**, 064615 (2008).
21. T. L. Belyaeva *et al.*, Phys. Rev. C 80, 064617 (2009).
22. I. J. Thompson, FRESCO user´s manual and code (available from author).
23. A. Gavron, Phys. Rev. C **21**, 1 (1980).
24. C. M. Perey, F. G. Perey, Atomic Data and Nuclear Data Tables **17**, 1-101 (1976).